Received: 5 May 2022 | Revised: 29 November 2022 | Accepted: 30 November 2022

DOI: 10.1002/biot.202200227

Biotechnology Journal

RESEARCH ARTICLE

Application of a split-Cre system for high-capacity adenoviral vector amplification

Manuela Gonzalez-Aparicio | **Maria Bunuales** | **Iñaki Ortiz de Landazuri** | **Jesus Prieto** | **Ruben Hernandez-Alcoceba**

University of Navarra, CIMA, Gene Therapy and Regulation of Gene Expression Program, Navarra Health Research Institute (IdiSNA), Pamplona, Spain

Correspondence
Ruben Hernandez-Alcoceba, University of Navarra, CIMA, Gene Therapy and Regulation of Gene Expression Program, Navarra Health Research Institute (IdiSNA), Av. Pio XII 55, E-31008 Pamplona, Spain.
Email: rubenh@unav.es

Funding information
CIMA-Transfiere CAN/Caixa Foundation; TERAV/ISCIII Next Generation, Grant/Award Number: EU-PRTR RD21/0017/0034

Abstract

Background and Aims: High-capacity adenoviral vectors (HC-AdV) show extended DNA payload and stability of gene expression in vivo due to the absence of viral coding sequences. However, production requires methods to trans-complement viral proteins, usually through Helper Viruses (HV). The Cre/loxP system is frequently employed to remove the packaging signal in HV genomes, in order to avoid their encapsidation. However, chronic exposure to the Cre recombinase in packaging cells is detrimental. We have applied the dimerizable Cre system to overcome this limitation.

Methods and Results: Cre was split in two fragments devoid of recombinase function (N-terminal 244 and C-terminal 99 amino-acids). In one version of the system, interaction with both moieties was favored by rapamycin-dependent heterodimerization domains (DiCre). Other version contained only Cre sequences (oCre). We generated packaging cells and HVs expressing the complementary fragments and studied their performance for HC-AdV production. We found that both conformations avoided interference with the growth of packaging cells, and the oCre system was particularly suitable for HC-AdV amplification.

Conclusions: The split-Cre system improves the performance of packaging cells and can reduce the time and cost of HC-AdV amplification up to 30% and 15%, respectively. This may contribute to the standardization of HC-AdV production.

KEYWORDS
dimerizable Cre, gene therapy, high-capacity adenovirus, recombinase, split-Cre

1 | INTRODUCTION

Viruses from the Adenoviridae family have been extensively adapted as gene therapy vectors. They are able to efficiently transduce a variety of cell types both in vitro and in vivo.[1] In order to avoid replication in the target cells, the early region E1 is removed from their genomes. In most vectors, the E3 region is partially or totally deleted as well, because it is dispensable for amplification in vitro. This leaves space for up to 8 Kb of exogenous DNA in these first-generation versions (FG-AdV). The E1 region can be efficiently complemented by packaging cells such as HEK-293 or equivalents, which support genome replication, late protein synthesis, encapsidation, and particle maturation.[2] Methods for affordable, high-scale production of

Abbreviations: CMV, cytomegalovirus; FG-AdV, first-generation adenoviral vector; HC-AdV, high-capacity adenoviral vector; iu, infectious units; min, minutes; vg, viral genomes; vp, viral particles.

clinical-grade FG-AdVs have been implemented. This has allowed the use of these vectors as vaccines against infectious diseases such as the Covid-19 pandemic.[3] However, FG-AdVs are not suitable for therapeutic applications requiring long-term expression of transgenes, since the residual expression of viral genes in the target cells triggers cellular immune responses against them.[4] To avoid this limitation and to increase the cloning capacity of adenoviral vectors, all viral coding genes were removed in the genome, giving rise to the High-Capacity Adenoviral vectors (HC-AdV), also called Helper-Dependent, third-generation or "*gutless*".[5]

Extensive preclinical work has demonstrated that HC-AdVs can deliver large genes or combination of genes efficiently in small and large animals. Importantly, expression can be sustained for long periods of time.[6] In principle, their cloning capacity reaches up to 36 to 37 Kb, which is enough to cover virtually all human monogenic diseases. However, clinical application of these vectors is hampered by the complexity of the production methods. Since all proteins needed for adenovirus amplification cannot be stably expressed in packaging cells, the standard procedure is based on the co-infection of the HC-AdV with a helper virus (HV). The HV is a FG-AdV which provides all viral proteins except for E1. The HV is not incorporated in the capsids because its packaging signal is flanked by sequences recognized by a recombinase expressed by the packaging cells. The packaging signal is thus cleaved only in the HV genome, whereas the HC-AdV genome can be encapsidated giving rise to infective particles. The most widely used method for cleavage is based on the Cre/LoxP system,[7–9] although alternatives employing other recombinases such as the Flp/FRT[10,11] or the Vika/vox[12] systems have been described. One current bottleneck is the need of packaging cells stably expressing not only E1, but also high levels of the recombinase.[13] This circumstance, initially described in the standard Cre/LoxP-based method, is potentially applicable to other systems. Cells expressing the recombinase suffer from genetic instability, resulting in slow and inconsistent growth rate.[14,15] This fact limits the reliability of production methods and increases its cost. The side effects associated with chronic exposure to Cre have been observed not only in cell cultures but also in vivo.[16–18] The mechanism could be the recognition of loxP-like sequences in the genome of mammalian cells.

Of note, Cre activity is highly efficient, which means that regulation at the level of protein expression is challenging. We have previously described a self-inactivating HV equipped with a drug-inducible expression system for Cre (AdTetCre).[19] In order to preserve the integrity of its genome, simultaneous control of protein expression and subcellular localization was needed. Still, the method requires expression of Cre in the packaging cells for optimal performance, and every AdTetCre batch requires thorough genetic and functional characterization to rule out selection of variants with defects of the expression cassette or the LoxP sites.

An alternative strategy to control Cre-mediated recombination is the use of the dimerizable or split-Cre systems. The method relies on the separation of the recombinase in two catalytically inactive moieties. In the original conception, the N- and C-terminal fragments are fused to complementary heterodimerization domains.[20] Treatment with dimerizing drugs such as rapamycin or analogs allows the specific interaction of protein fragments and the reconstitution of the recombinase function. Other ways to ensure re-assembly of the protein include the use of overlapping fragments or the addition of split-inteins. Interestingly, it has been reported that the reassembly of some Cre segments is possible in the absence of additional dimerization domains.[21]

In this work we have used the split-Cre system to obtain scission of the packaging signal from the HVs in the absence to chronic exposure to the recombinase in either the packaging cells or the HV itself.

2 | EXPERIMENTAL SECTION

No animal experimentation or human studies have been performed in this work.

2.1 | Plasmid construction

Cloning was carried out using standard molecular biology techniques utilizing enzymes from New England Biolabs (Ipswich, MA, USA), unless otherwise stated. T4 DNA ligase was from Promega (Madison, WI, USA). DmrA and DmrC heterodimerization domains were obtained from the pHet-Actl-2 plasmid (Clontech-Takara, Mountain View, CA, USA). Fusions with Cre domains were synthetized by GenScript (Piscataway, NJ, USA). pBS185 (referred to here as pCre343) is a plasmid expressing the full Cre recombinase under the control of the CMV promoter (Addgene #11916).[22] The reporter plasmid pLoxPLuc contains the Firefly luciferase gene under the control of the SV40 promoter and flanked by loxP sites. HV genomes are based on pAdEasy-1 plasmid,[23] a plasmid harboring deletions of the E1 and E3 regions in the human adenovirus type 5 (HAdVC5) genome. The packaging signal was flanked by loxP sites. The standard HV Ad-KE3 contains no expression cassettes, but the E3 region was re-introduced (plasmid pAd-KE3). The CMV-DiCre99 expression cassette was introduced into the unique SwaI site of pAd-KE3 to give rise to the pAd-DiCre99 plasmid. The pAd-oCre99 plasmid contains two expression cassettes. The CMV-oCre99 cassette was introduced into the SwaI site, whereas a cassette comprising the Elongation Factor 1α promoter, the beta-galactosidase (LacZ) coding sequence and a poly-adenylation signal was introduced into the unique BstBI site. The E3 region was eliminated to keep the genome size below 37 Kb. The genome of the HC-AdV vector pHCA-EGFP has been previously described.[19] It contains a CMV-enhanced GFP cassette and human-derived stuffer DNA.

2.2 | Cell culture

HEK-293 cells (ATCC#CRL-1573, ATCC, Rockville, MD, USA) were cultured in Dulbeccot's modified Eagle medium (DMEM) (Invitrogen/Life Technologies, Waltham, MA, USA) supplemented with 10% fetal bovine serum (FBS) (Gibco-Thermo Fisher Scientific, Waltham, MA, USA); 100 U mL^{-1} penicillin, 100 U mL^{-1} streptomycin, and 2 mM L-glutamine. Detachment of cells was performed by incubation with saline cit-

rate (134 mM Potassium Chloride, 15 mM Sodium Citrate, Sigma St. Louis, MO, USA). All cells were routinely tested for Mycoplasma contamination and maintained at 37°C with 8% CO_2 in a humidified incubator. For the generation of cells stably expressing the DiCre244 and oCre244 proteins, transfection was performed in 2.5×10^5 HEK-293 cells seeded on 24-well plates, using 1 μg/well of plasmid and 2 μl/well lipofectamine 2000 (Thermo Fisher Scientific, Waltham, MA, USA). Forty-eight hours after transfection, wells were subcultured on a 100 mm plate. The selection antibiotic Hygromycin (0.1 mg mL^{-1}) was added 3 days after plating, and cell colonies were manually isolated. Selected clones were maintained with the same dose of antibiotic in the growth medium. The standard packaging cells for HC-AdV production with stable expression of the full Cre recombinase (293Cre4),[7,24] referred hereinafter as 293-Cre, were maintained with 400 μg mL^{-1} geneticin (G418, Invitrogen/Life Technologies, Waltham, MA, USA) in the growth medium. Doubling times for each cell line were calculated using Roth V. 2006 Doubling Time Computing, Available from: http://www.doubling-time.com/compute.php.

2.3 | Virus production and quantification

Initial batches of HVs were produced by transfection of the respective plasmids in HEK-293 cells using lipofectamine 2000. Once the cytopathic effect was observed (usually 7 to 12 days after transfection), cell lysates were obtained by three rounds of freezing and thawing and subsequent centrifugation at 2.500 rpm for 5 min. Viruses released into the supernatant were cloned by end-limiting dilution. Amplification of selected clones was performed in HEK-293 cells.

For HC-AdV production, vector genomes (obtained by linearization of plasmids) were initially transfected in the corresponding packaging cells, and 4 to 6 h later cells were infected with the HV at multiplicity of infection (MOI) of 1 infectious unit (iu)/cell. Cell lysates obtained 48 h later by three consecutive cycles of freeze-thaw in liquid Nitrogen were used for infection of cells in the next step, together with HV at MOI 1. 293-DiCre244 cells were treated with 500 nM rapamycin. For the amplification process, the number of cells was only increased when the previous step obtained transduction of at least 90% of cells, determined by GFP expression (see the result section for details of each HV/packaging cell system). Purification of HVs was carried out by double CsCl density gradient ultracentrifugation (Roche, Indianapolis, IN, USA). For quantification of viral particles (vp), samples were treated with 10% SDS for 10 min and the absorbance at 260 nm was measured in a spectrophotometer, as previously described.[25] Quantification of iu of HVs was done using the Adeno-X rapid titer kit (Clontech-Takara, Mountain View, CA, USA), and verified by end-limiting dilution cytopathic assay in HEK-293 cells. In the case of HCA-EGFP, iu were quantified by detection of GFP^+ cells in the same type of cells (transducing units). To this end, HEK-293 cells were infected with serial dilutions of the vector in 24-well plates. GFP^+ cells were counted under a fluorescence microscope. Wells with up to 20 cells/field were used for calculation of viral titers.

2.4 | Analysis of Cre function

HEK-293 cells were co-transfected with the reporter plasmid pLox-PLuc and the plasmids encoding different Cre fragments. Forty-eight hours later, cells were collected and resuspended in 200 μL of PBS. Plasmid DNA was extracted using QIAamp DNA Mini Kit (Qiagen). Endpoint PCR was performed from DNA samples using primers P1 (5′ TTCCGCCCATTCTCCGCC 3′) and P3 (5′ TCTTATCATGTCTGCTCGAAGCGG 3′) with 55°C annealing temperature and 35 cycles. PCR products were resolved in a 1.5% agarose gel to detect the 201 bp band resulting from Cre-mediated cleavage. Fragment size was determined by comparison with the 1 Kb Plus DNA ladder (Invitrogen/Life Technologies, Waltham, MA, USA).

2.5 | X-Gal staining

For analysis of β-Galactosidase activity, cell monolayers were fixed for 10 min in a solution containing 0.5% (w/w) glutaraldehyde in PBS. The fixative was then removed and the cells were covered with staining solution (1 mg mL^{-1} X-Gal, Gibco; 1 mM $MgCl_2$; 5 mM $K_3Fe(CN)_6$; and 5 mM $K_4Fe(CN)_6$ in PBS) and incubated at 37°C for 1 to 4 h.

2.6 | Western blot

Cells cultured in 6-well plates were detached by pipetting, washed with PBS and centrifuged at 1.500 rpm for 5 min at 4°C. Dry pellets were frozen at -80°C and then resuspended in 100 μl lysis buffer (Tris-HCl 10 mM pH 7.4, SDS 2%, PMSF 1 mM, Aprotinin 1 μg mL^{-1}, Na_3VO_4 1 mM, $Na_4P_2O_7$ 1 mM, 10% β-Mercaptoethanol vol:vol and 1x Laemmli Sample Buffer from Bio-Rad). Samples were sonicated 5 to 10 min at 4°C and then boiled at 95°C for 5 min. Twenty μl were loaded into the acrylamide gel (4% to 15% Mini-PROTEAN TGX Precast Protein Gel Bio-Rad). Proteins were transferred to a nitrocellulose membrane (Bio-Rad) and blocked with 5% BSA in TBS-Tween 1%. Incubation with the primary antibody (1:5.000 rabbit polyclonal anti-Cre, BioLegend or 1:5.000 rabbit monoclonal anti-GAPDH, Cell Signaling) was performed overnight in TBS-Tween 1% with 1% BSA at 4°C. Incubation with the secondary antibody (1:10.000 goat anti-rabbit IgG conjugated with alkaline phosphatase, Abcam) was performed at room temperature for 1 h. Detection was carried out using the ECL Ultra (TMA-6) reagent from Lumigen. Images were obtained in the Odyssey XF Dual-Mode Imaging System.

2.7 | Statistical analysis

Comparison of two groups was performed using the Mann-Whitney test. Three or more groups were compared using the Kruskal-Wallis test followed by the Dunn's multiple comparisons test, or the parametric test ANOVA with Tukey's multiple comparisons test if the values show normal distribution. Amplification curves of cells and viruses

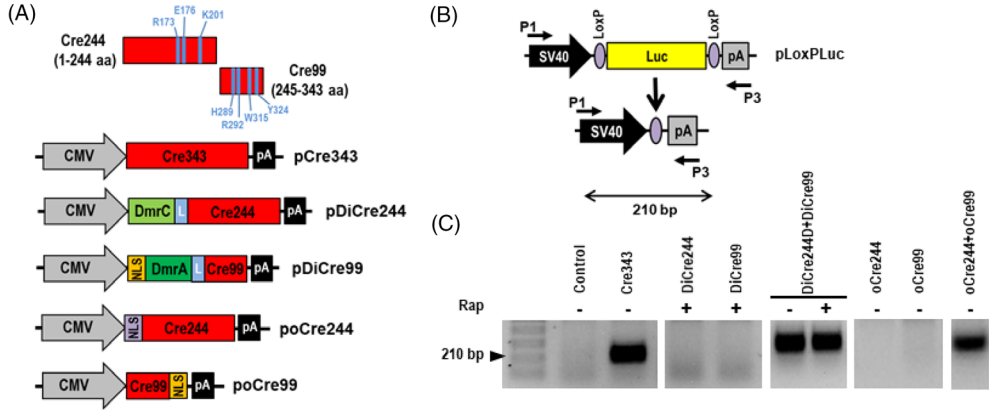

FIGURE 1 **Cre fragments reconstitute recombinase activity upon co-expression in packaging cells. (A)** Schematic representation of plasmids encoding dimerizing and split Cre versions. pCre343 refers to the plasmid encoding the full Cre recombinase sequence under the control of the CMV promoter. Cre244 and Cre99 refer to the N-terminal (1 to 244) and C-terminal (245 to 343) amonoacids of Cre, respectively. In the top image, the location of amino acids conforming the active site is indicated by blue lines. DmrC and DmrA are rapamycin-dependent heterodimerization domains. NLS, nuclear localization signals from human c-Myc (DiCre99 and oCre99), or SV40 large-T antigen (oCre244). L, peptide linker. pA, polyadenylation signal. **(B)** Schematic representation of the pLoxPLuc reporter plasmid and the PCR method employed to analyze recombinase function. Luc, luciferase sequence. P1 and P3, primers used for PCR analysis. The Cre-mediated cleavage of luciferase results in a 210 bp-long PCR fragment. **(C)** The indicated plasmids were co-transfected with pLoxPLuc in HEK-293 cells. When indicated, cells were treated with rapamycin (Rap+). Forty-eight hours later cell extracts were collected for isolation of plasmid DNA and PCR analysis using the P1 and P3 primers. A representative agarose gel is shown. The left line corresponds to the 1 Kb Plus DNA ladder from Invitrogen. pcDNA3.1 was used as a negative control

were compared by linear regression analysis. All graphs and tests were performed using the GraphPad 6 Prism software (GraphPad, La Jolla, CA, USA).

3 | RESULTS

3.1 | Cre fragments with incomplete active site are devoid of recombinase activity but can recover it upon co-expression in packaging cells

In order to ensure the absence of recombinase activity in the individual Cre fragments, we used one sequence encoding amino acids 1–244 (Cre244) and another one encoding amino acids 245–343 (Cre99). This conformation guarantees a strict separation of amino acids conforming the active site,[26] since R173, E176, and K201 remain in Cre244, whereas H289, R292, W315, and Y324 are located in Cre99 (Figure 1A), as previously described.[21] Conditional interaction between both moieties was favored by fusion of heterodimerization domains derived from human FKBP12 and the FKBP12-associated protein FRAP (mTOR), designated DmrA and DmrC, respectively. Rapamycin binds to the FKBP12 domain, and then the FKBP12-rapamycin complex binds to FRAP. A nuclear localization signal (NLS) derived from the human c-Myc gene (PAAKRVKLV)[27] was added at the N-terminal portion of the Cre99 fragment (DiCre99), whereas DiCre244 contains the endogenous NLS from the recombinase.[28] For functional evaluation, plasmids encoding these fusion proteins were transfected in the packaging cells HEK-293, alone or in combination. In all cases, cells were simultaneously transfected with a reporter plasmid (pLoxPLuc) in which the luciferase coding sequence is flanked by loxP sites (Figure 1B). If the recombinase activity is restored, the 1.6 Kb-long luciferase sequence is cleaved, and the primers specific for the promoter and the polyadenylation signal generate a PCR product of 210 bp in length, which is easily detected in an agarose gel. As a positive control, cells were transfected with a plasmid encoding the full Cre sequence (pCre343). As expected, transfection of this plasmid generated a strong PCR band (Figure 1C), whereas the individual pDiCre244 and pDiCre99 plasmids caused no luciferase cleavage. Co-transfection of these plasmids efficiently restored the recombinase activity. Surprisingly, the cleaved product was also detected in the absence of rapamycin treatment, suggesting that the heterodimerization domains are not required for reconstitution of the Cre activity, in line with previous results generated in plant cells.[21] Therefore, we generated a pair of plasmids encoding only the Cre fragments (oCre244 and oCre99), with addition of a NLS from the SV40 Large-T antigen (DPKKKRKVDPKKKRKV) and the human c-Myc gene, respectively (Figure 1A). The function of these constructs was tested using the pLoxPLox reporter plasmid. We confirmed that these Cre fragments show recombinase activity only when they are co-transfected in the packaging cells (Figure 1C). Although the mechanism of spontaneous re-assembly has not been elucidated, it may depend on the extensive protein-DNA interface between Cre and the loxP sequence,[29] which favors the functional interaction of fragments around the DNA.

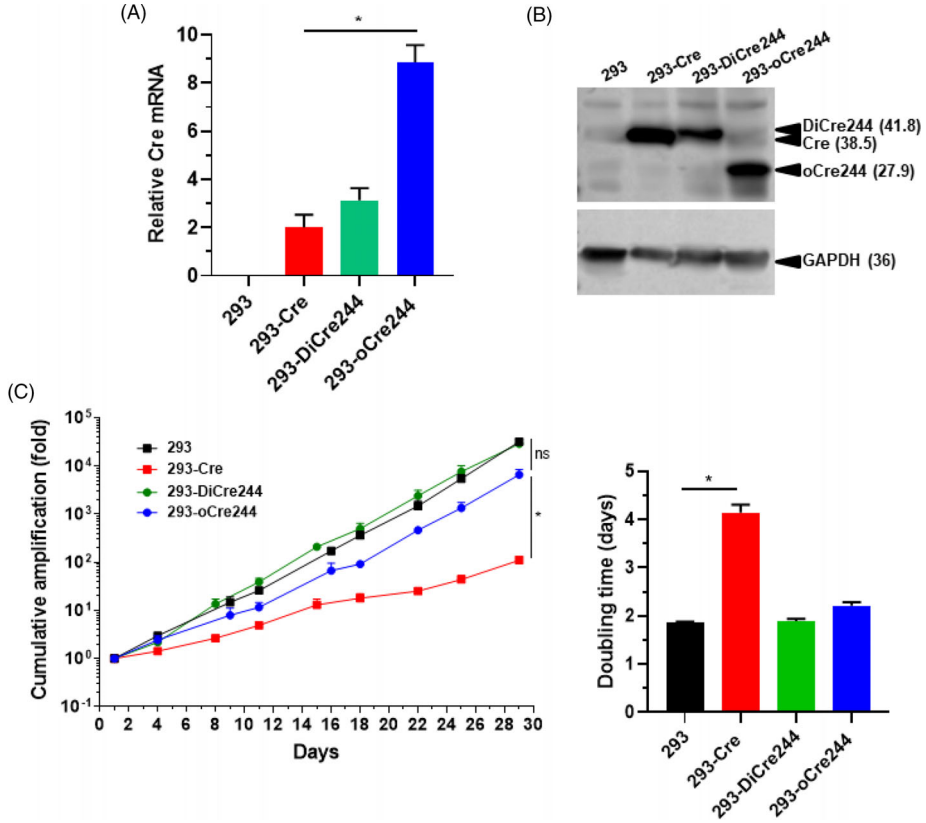

FIGURE 2 **Stable expression of DiCre244 and oCre244 does not impair the growth of HEK-293 cells. (A)** Expression of Cre variants in the indicated cells, determined by qRT-PCR using primers specific for the N-terminal portion of the coding sequence. 293 refer to the parental HEK-293 cells without expression of Cre. Values correspond to the relative mRNA content, using 36b4 as a reference ($2^{\Delta Ct\,(36b4\text{-}Cre)}$). *$p < 0.05$, Kruskal-Wallis with Dunn's post-test. **(B)** Western blot for detection of Cre protein variants. The predicted molecular weights are indicated in parenthesis. GAPDH was used as a housekeeping gene as a reference of cell content in the lysates (bottom panel). The picture shows representative samples from triplicates. **(C)** Quantification of cell expansion over time. Left, fold increase in the number of cells relative to the initiation of the experiments (day 0). *$p < 0.05$, linear regression analysis. Right, doubling time for each cell line. *$p < 0.05$, Kruskal-Wallis test

3.2 | Stable expression of DiCre244 and oCre244 does not impair the growth of HEK-293 cells

Once the function of the two dimerizable Cre versions was confirmed in HEK-293 cells, we produced cell lines stably expressing the DiCre244 and oCre244 sequences. Clones with the highest expression of each Cre moiety were selected (not shown). When expression was compared across different packaging cells by qRT-PCR, we found similar levels in 293-DiCre244 cells and a standard packaging cell line expressing the full Cre recombinase (293-Cre).[7,24] Expression of the Cre244 fragment in the 293-oCre244 cells was significantly higher at the mRNA level (Figure 2A), but detection of protein content by Western blot revealed no differences (Figure 2B). The growth kinetics of the three Cre-expressing cells were compared with the parental HEK-293 cells during 1 month. Figure 2C shows the cumulative amplification of cells obtained at different times, and the doubling times. As expected, chronic exposure to the active Cre recombinase in 293-Cre cells resulted in a reduction of proliferative rate, whereas 293-DiCre244 and 293-oCre244 showed no significant differences from the parental cells. Only a tendency towards a slight growth delay was observed in the case of 293-oCre244 cells.

3.3 | Reconstitution of Cre activity between customized HVs and packaging cells allows efficient control of HV production

The expression cassettes containing the DiCre99 and oCre99 sequences were incorporated in FG-AdVs. Their packaging signal was flanked by loxP sites in order to make them susceptible to cleavage by Cre, giving rise to the new Ad-DiCre99 and Ad-oCre99 HVs (Figure 3A). Expression of the respective Cre variants was demonstrated by Western blot upon infection of HEK-293 cells (Figure 3B). However, quantitative comparisons among them are not possible because the polyclonal antibodies available could have lower affinity for the shorter Cre99 fragment due to limited epitope abundance. An expression cassette for the reporter gene LacZ was inserted in Ad-oCre99 in order to facilitate quantification of transduction units by β-Galactosidase reaction. This can be useful at preclinical stages in order to asses if HV contamination in the final HC-AdV batches is relevant at the level of cell transduction in vitro and in vivo. Production of the new HVs was carried out following standard procedures in HEK-293 cells. The viability of Ad-DiCre99 and Ad-oCre99 indicates that the Cre99 fragment alone is unable to cleave

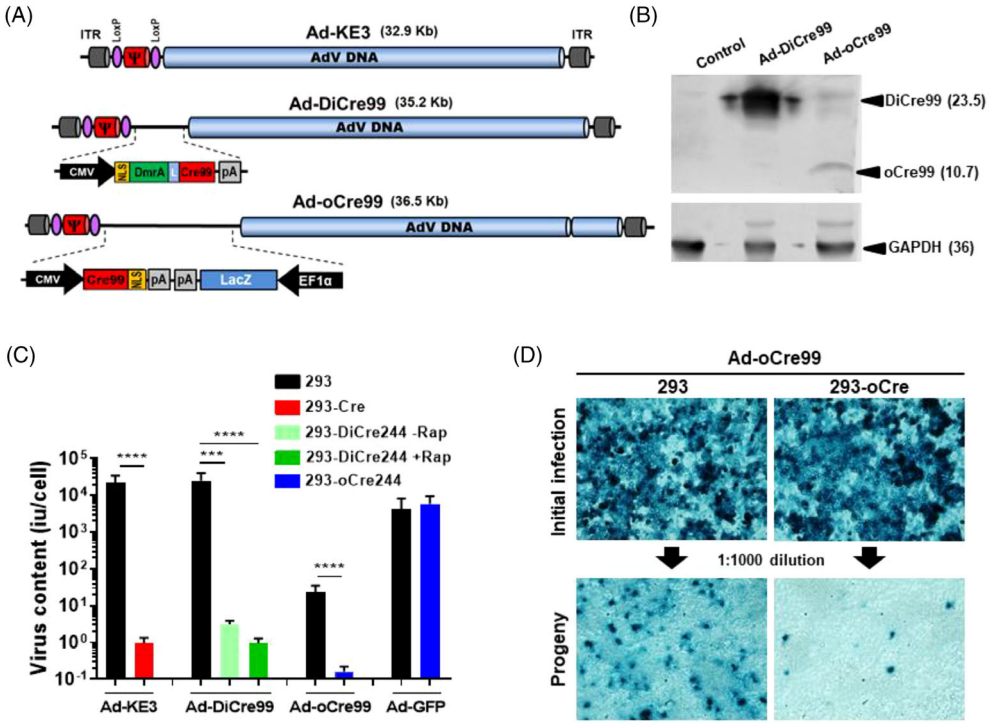

FIGURE 3 **Inactivation of Adenovirus production by split-Cre. (A)** Schematic representation of the genomes of HVs. Ad-KE3 is the standard virus with the packaging signal (Ψ) flanked by loxP sites. Ad-DiCre99 and Ad-oCre99 express the DiCre99 and oCre99 polypeptides (respectively) under the control of the CMV promoter. Ad-oCre99 contains an additional expression cassette including the LacZ gene under the control of the Elongation Factor 1 α promoter (EF1α). Not drawn to scale. **(B)** HEK-293 cells were infected with the indicated HVs at MOI 2, and cell extracts were obtained 48 h later for identification of Cre fragments by Western blot. The predicted molecular weight is indicated in parenthesis. GAPDH was used as a housekeeping gene for control of cell content in the lysates (bottom panel). The picture shows representative samples from triplicates. **(C)** The indicated cells were infected with Ad-KE3, Ad-DiCre99, or Ad-oCre99 HVs, and 48 h later the production of infective particles was quantified (expressed as iu/cell). **(C)** HEK-293 and 293-oCre244 cells were infected with Ad-oCre99 at MOI 1. Forty-eight hours later, cells expressing LacZ were identified by X-Gal staining (blue color) in a subset of wells to determine the initial transduction rate. In the remaining wells, cell lysates were obtained, diluted 1:1000 in growth medium and added to fresh HEK-293 cells. Transduced cells were identified 48 h later by X-Gal staining (blue color). *** $p < 0.001$; **** $p < 0.0001$, Mann-Whitney U test

the packaging signal, even in the context of genome replication, when expression levels are maximized. This is in sharp contrast with the full Cre recombinase.[19] When viral progeny production of the vectors was compared between HEK-293 and the customized packaging cells, a strong reduction (more than 99%) was observed (Figure 3C). This is not due to inefficient transduction of the cells, as shown in Figure 3D. The limitation of HV progeny production is equivalent to that observed with a standard HV (Ad-KE3) in 293-Cre cells. As expected, the addition of rapamycin caused only a marginal reduction in the production of the Ad-DiCre99 vector in 293-DiCre244 cells, supporting the notion that both Cre subunits can interact spontaneously. Interestingly, production of Ad-oCre99 in HEK-293 cells was lower than the other HVs (Figure 3C), which raised concerns about its performance during the process of HC-AdV amplification. Of note, the strong inhibition of Ad-oCre99 in 293-oCre244 cells is not due to a general reduction of the permissiveness of the cells, since they can efficiently support the amplification of a standard FG-AdV (Ad-GFP, Figure 3C).

3.4 | The use of dimerizable Cre increases the efficiency of HC-AdV production

In order to validate the function of the new HV/packaging cell systems, we employed them for amplification of a representative HC-AdV expressing eGFP (HCA-EGFP).[19] The conventional system based on Ad-KE3 and the 293-Cre cells was used as a reference. The initial phase (step 0) is common to all protocols and consists of the transfection of the HCA-EGFP genome and subsequent infection with the HV in a 60 mm cell culture plate. The amplification protocol was tailored to obtain progressive enrichment of HC-AdV. To this end, the percentage of transduced (GFP^+) cells in the plate was determined 48 h after infection, and the number of cells in the next step was only increased if more than 90% cells were transduced. Using this setting, the conventional system required an additional enrichment step in 60 mm (p60) cell culture plates after transfection, before the scale-up to a p100 plate with 9×10^6 cells was possible. From this step, two additional rounds of amplification (10-fold number of cells each) were performed

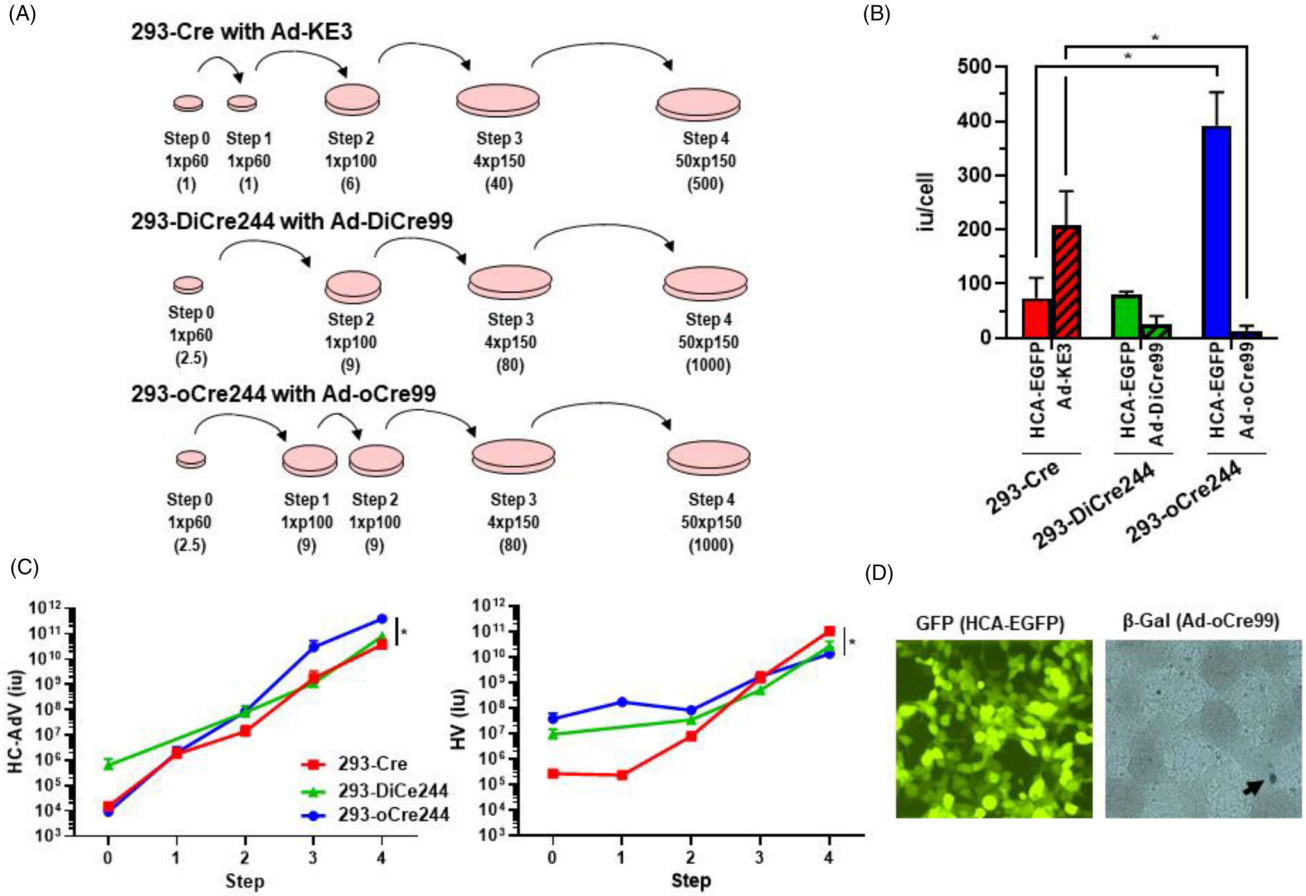

FIGURE 4 **The use of split-Cre increases the efficiency of HC-AdV production. (A)** Schematic representation of the amplification process, indicating the number and size of cell culture plates in each step, with the total number of cells (millions) in parenthesis. The HC-AdV corresponds to HCA-EGFP. See Materials and Methods section for details. **(B)** Quantification of HC-AdV yield and HV accumulation in cell lysates obtained after the last amplification step using the indicated packaging cells. The values correspond to iu/cell of the HC-AdV (HCA-EGFP) or the specific HVs Ad-KE3, Ad-DiCre99, and Ad-oCre99, depending on the system. HC-AdV is represented in plain columns and HVs are represented in striped columns. **(C)** Progression of HC-AdV and HV amplification (in total iu) in each step. **(D)** Representative image of HEK-293 cells infected at MOI 2 with the HCA-EGFP vector obtained with the oCre system. The left picture corresponds to fluorescence microscopy showing GFP^+ cells transduced with HCA-EGFP (green). The right picture corresponds to X-Gal staining showing LacZ-expressing cells transduced with Ad-oCre99 (blue cell, arrow). $^*p < 0.05$, Mann-Whitney U test

in p150 plates until the laboratory-scale batch was obtained, corresponding to 50 plates with a total number of 5×10^8 for 293Cre cells and 1×10^9 for 293-DiCre244 and 293-oCre244 cells (Step 4, Figure 4A). Using the 293-DiCre244/Ad-DiCre99 system (DiCre system), enrichment in HCA-EGFP was faster, and Step 1 in the second p60 plate could be omitted. Finally, the 293-oCre244/Ad-oCre99 system (oCre system) required enrichment at the level of the p100 plates (Steps 1–2). Cell lysates obtained from the last step were used to quantify infectious units of HCA-EGFP and the respective HVs. Compared with the standard method, only the oCre system achieved a significant increase of HCA-EGFP yield combined with lower HV contamination (Figure 4B and Table 1). This is consistent with the efficient inhibition of Ad-oCre99 production in 293-oCre244 cells observed in Figure 3D, and suggest that a relatively low progeny burst size in HEK-293 cells is not detrimental to exert its helper function. The progress of HCA-EGFP and HV amplification in the three systems is illustrated in Figure 4C. The fast enrichment in HCA-EGFP obtained with the DiCre system is evident during the first steps, whereas oCre and the standard system follow a slower but consistent progression of HC-AdV accumulation. Regarding HV, 293-Cre cells exerted an efficient control of Ad-KE3 only during the first 2 steps of amplification, but afterwards the accumulation goes in parallel with HCA-EGFP (Figure 4C). This does not correlate with a simultaneous loss of Cre expression in cultured cells, as shown in Figure S1. In contrast, the oCre system maintained the restriction of Ad-oCre99 production during all the process and kept the contamination percentage below 5% in the crude lysates at step 4. Incorporation of the LacZ expression cassette allows direct functional evaluation of Ad-oCre99 contamination in cell culture. When the HCA-EGFP vector produced with the oCre system was used to infect HEK-293 cells at MOI 2, 100% cells express GFP, whereas only a few cells are positive for X-Gal staining (Figure 4D). More importantly, a clear advantage of the new system is the efficacy and reliability of packaging cell growth, which accelerates the process and optimizes the use of cell culture materials (Table 1). To further characterize the function

TABLE 1 Parameters of HC-AdV amplification using the indicated systems. Values correspond to cell lysates obtained in step 4 (50 p150 plates), resuspended in 7 mL culture medium (average of 3 independent amplifications ± SD). Infectious units of HC-AdV and HV were quantified in HEK-293 cells by direct GFP visualization and immnunohistochemistry for late AdV proteins, respectively. The time and materials include all intermediate cultures needed to obtain the required number of cells for the four amplification steps

System	HC-AdV yield (total iu x 10^{10})	HV accumulation (total iu x 10^{10})	Time (days)	Cell culture plates (p150)	Cell culture medium [mL]
Standard	5.15 ± 2.84	13.55 ± 0.49	47	113	2960
DiCre	7.96 ± 1.05	2.61 ± 2.52	28	91	2610
OCre	39.23 ± 10.63	1.31 ± 1.67	35	96	2652

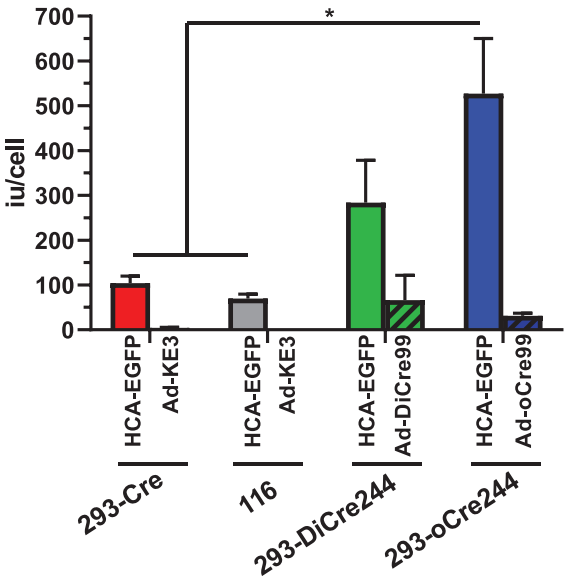

FIGURE 5 **Single round amplification of HC-AdV and HV in different packaging cells**. The indicated cells were co-infected with the HCA-EGFP vector at MOI 5 and the HV specific for each production system at MOI 1. Cell lysates were obtained 48 h later for quantification of HC-AdV amplification and HV accumulation. The values correspond to iu/cell of HCA-EGFP or the specific HVs Ad-KE3, Ad-DiCre99, or Ad-oCre99, depending on the system. HCA-EGFP is represented in plain columns and HVs are represented in striped columns. $^{*}p < 0.05$, ANOVA with Tukey's multiple comparisons test

of the systems, purified HCA-EGFP vector produced by each method was co-infected with the corresponding HV at a defined ratio in the different packaging cells (MOI 5 for vector and MOI 1 for HV). Apart from 293-Cre, we included the 116 packaging cell line as additional example of constitutively expressed Cre recombinase.[30] Of note, the proliferation rate of 116 is reduced in comparison with HEK-293 cells (Figure S2), as observed in 293-Cre. Cell lysates were obtained 48 h after infection of each cell line for the quantification of HC-AdV and HV generated in a single cycle (progeny burst size, expressed as infectious unit/cell). In agreement with the previous results, the oCre system produced more HC-AdV than the others (Figure 5). All systems were able to control HV production in a single cycle, although the 293-Cre cells accumulated more HV at the end of the amplification process (Figure 4B).

4 | DISCUSSION

HC-AdVs offer unique opportunities in the field of gene therapy.[9] However, technical improvements in production methods are needed to expedite their clinical implementation. The use of the Cre/loxP system for removal of the packaging signal in HVs has been extensively validated during the last 3 decades. A delicate balance exists between the amount of recombinase needed to process a high number of HV genomes on one side, and the deleterious effects on packaging cells on the other side. So far, this problem has been circumvented by empirical selection of cells.[30]

Our results show that customized pairs of HV and packaging cells expressing complementary Cre fragments can increase the reliability of the method for HC-AdV production. Using this system, the fragments can be expressed at high levels without compromising the integrity of either vectors or cells, because the functional recombinase will only be active during the process of HC-AdV amplification, when the HV exerts its trans-complementing function in the specific packaging cells. Only during this step, the interference with HV encapsidation is beneficial, and the cells do not need to continue proliferating. Therefore, packaging cells can be amplified with optimal growth rates and are protected from eventual collapse, which is frequently observed during long-term maintenance of conventional Cre-expressing cells.

Based only on the improvement of cell growth, our conservative estimation is that the amplification process of HC-AdVs can be accelerated close to 30%, and the use of materials can be reduced by 10% to 15%. These features could be instrumental for the establishment of continuous multi-stage bioreactors for HC-AdV production.[31] Regarding quality parameters such as HV contamination, further work is needed to establish meaningful comparisons with other systems. Of note, we have used crude lysates for characterization, in order to exclude the influence of different purification options. It should be considered that a significant fraction of HV can be removed during purification.[7,33] This may explain why we have detected relatively high HV contamination percentages, especially in the case of the standard system. In addition, we have used a stringent and functionally relevant method to calculated these percentages, based on quantification of transducing units of HC-AdV and HV in HEK-293 cells. In contrast, methods relying solely on viral genome (vg) quantification may underestimate HV contamination because the vg:iu ratio is usually higher in HC-AdVs than HVs. Another factor that could contribute to the high HV accumulation in the case of our 293-Cre cells is the down-

regulation of Cre expression as an adaptation to long-term culture maintenance, although this phenomenon does not take place during the 4 to 6 weeks required for the amplification of a particular vector batch (Figure S1). In any case, we cannot rule out the possibility that the original 293Cre4 stocks, and especially other improvements developed afterwards,[8,30,32] could be more efficient in HV removal. However, we believe our results are valid to demonstrate the advantage of the split-Cre system versus chronic expression of the native recombinase.

Although only speculative, a reduced viral fitness of Ad-oCre99 could contribute to control contamination with this HV and could provide a relative advantage for HC-AdV amplification. The reduced fitness could be due to the extension of genome size obtained after insertion of the LacZ expression cassette (36.595 bp, which exceeds 1.8% the genome of the wild type HAdVC5 virus). Although extensions up to 5% of genome size are tolerated,[34] encapsidation efficacy could be slightly compromised. As far as this effect does not impair production of the vector or its trans-complementing function as a HV, this is a desirable trait. An alternative explanation is that the oCre99 fragment could present residual Cre activity, but we have no evidence supporting this possibility. In the same vein, a slight, non-significant reduction of growth rate was observed in 293-oCre244 cells versus 293-DiCre244 or the parental HEK-293 cells. However, we cannot attribute this effect to residual Cre function of the Cre244 moiety. If this was the case, the addition of dimerizable domains to the Cre99 and Cre244 moieties seems to avoid this effect, maybe because they increase the size of the proteins and reduce their nuclear import. Although comparison of the two dimerizable Cre-based systems is not straightforward, the oCre system provides a convenient equilibrium between efficacy and stability of its components.

This is a proof of concept study performed with widely accessible packaging cells and HVs without additional optimizations in the packaging signal or other elements. We have only characterized the HC-AdV amplification process in a laboratory scale using attached cells. Comparison with other systems is not the objective of this work. This is not straightforward because characterization of crude lysates is seldom reported in the literature, quantification may be different, and the values are highly influenced by the experimental conditions employed. Notwithstanding, the yield we obtained with the oCre system (392 iu/cell, Figure 4B) is within the range described by other groups using adherent 116 cells during the amplification process.[8,32] We believe that the concept can be applied to the most advanced systems based on improved cells, HVs, growth conditions and purification processes, which are usually proprietary materials of biotech companies. The potential adaptation of the system to recombinases different from Cre depends on the feasibility functional split versions.

In conclusion, the method described here can improve the production of HC-AdVs and facilitate its standardization and adaptation to good manufacturing practice (GMP) conditions for clinical use.

AUTHOR CONTRIBUTIONS

Manuela Gonzalez-Aparicio: Data curation; Investigation; Methodology; Writing – review & editing. Maria Bunuales: Methodology. Iñaki Ortiz de Landazuri: Methodology. Jesus Prieto: Conceptualization; Investigation; Supervision. Ruben Hernandez-Alcoceba: Conceptualization; Data curation; Funding acquisition; Investigation; Resources; Supervision; Writing – original draft.

MGA, MB, and IOL performed the experiments; RHA conceived the study, obtained funding and wrote the manuscript; RHA, MGA and JP designed the experiments and analyzed the data; MGA revised the manuscript.

ACKNOWLEDGMENTS

This project was funded by CIMA-Transfiere CAN/Caixa Foundation (VEASID) and TERAV/ISCIII Next Generation EU-PRTR RD21/0017/0034.

CONFLICT OF INTEREST

The authors declare no conflicts of interest.

DATA AVAILABILITY STATEMENT

Raw data have been deposited in Zenodo (DOI: 10.5281/zenodo.7376148).

ORCID

Ruben Hernandez-Alcoceba https://orcid.org/0000-0002-6682-2598

REFERENCES

1. Gao, J., Mese, K., Bunz, O., & Ehrhardt, A. (2019). Stateâofâtheâart human adenovirus vectorology for therapeutic approaches. *Febs Letters*, *593*(24), 3609–3622. https://doi.org/10.1002/1873-3468.13691
2. Graham, F. L., Smiley, J., Russell, W. C., & Nairn, R. (1977). Characteristics of a human cell line transformed by DNA from human adenovirus type 5. *Journal of General Virology*, *36*(1), 59–72. https://doi.org/10.1099/0022-1317-36-1-59
3. Mendonça, S. A., Lorincz, R., Boucher, P., & Curiel, D. T. (2021). Adenoviral vector vaccine platforms in the SARS-CoV-2 pandemic. *Npj Vaccines*, *6*(1). https://doi.org/10.1038/s41541-021-00356-x
4. Yang, Y., Ertl, H. C. J., & Wilson, J. M. (1994). MHC class I-cestricted cytotoxic T lymphocytes to viral antigens destroy hepatocytes in mice infected with E1-deleted recombinant adenoviruses. *Immunity*, *1*(5), 433–442. https://doi.org/10.1016/1074-7613(94)90074-4
5. Ricobaraza, A., Gonzalez-Aparicio, M., Mora-Jimenez, L., Lumbreras, S., & Hernandez-Alcoceba, R. (2020). High-capacity adenoviral vectors: Expanding the scope of gene therapy. *International Journal of Molecular Sciences*, 21(10). https://doi.org/10.3390/ijms21103643
6. Brunetti-Pierri, N., Ng, T., Iannitti, D., Cioffi, W., Stapleton, G., Law, M., Breinholt, J., Palmer, D., Grove, N., Rice, K., Bauer, C., Finegold, M., Beaudet, A., Mullins, C., & Ng, P. (2013). Transgene expression up to 7 years in nonhuman primates following hepatic transduction with helper-dependent adenoviral vectors. *Human Gene Therapy*, *24*(8), 761–765. https://doi.org/10.1089/hum.2013.071
7. Parks, R. J., Chen, L., Anton, M., Sankar, U., Rudnicki, M. A., & Graham, F. L. (1996). A helper-dependent adenovirus vector system: Removal of helper virus by Cre-mediated excision of the viral packagingâ‰signal. *Proc. Natl. Acad. Sci. U.S.A.*, *93*(24), 13565–13570. http://www.ncbi.nlm.nih.gov/entrez/query.fcgi?cmd=Retrieve&db=PubMed&dopt=Citation&list_uids=8942974
8. Ehrke-Schulz, E., Zhang, W., Schiwon, M., Bergmann, T., Solanki, M., Liu, J., Boehme, P., Leitner, T., & Ehrhardt, A. (2016). Cloning and large-scale production of high-capacity adenoviral vectors based on the human adenovirus type 5. *Journal of Visualized Experiments*, *2016*(107), 1–15. https://doi.org/10.3791/52894

9. Brücher, D., Kirchhammer, N., Smith, S. N., Schumacher, J., Schumacher, N., Kolibius, J., Freitag, P. C., Schmid, M., Weiss, F., Keller, C., Grove, M., Greber, U. F., Zippelius, A., & Plückthun, A. (2021). iMATCH: An integrated modular assembly system for therapeutic combination high-capacity adenovirus gene therapy. *Molecular Therapy – Methods and Clinical Development*, *20*, 572–586. https://doi.org/10.1016/j.omtm.2021.01.002
10. Umana, P., Gerdes, C. A., Stone, D., Davis, J. R., Ward, D., Castro, M. G., & Lowenstein, P. R. (2001). Efficient FLPe recombinase enables scalable production of helper-dependent adenoviral vectors with negligible helper-virus contamination. *Nature Biotechnology*, *19*(6), 582–585. http://www.ncbi.nlm.nih.gov/entrez/query.fcgi?cmd=Retrieve&db=PubMed&dopt=Citation&list_uids=11385466
11. Ng, P., Beauchamp, C., Evelegh, C., Parks, R., & Graham, F. L. (2001). Development of a FLP/frt system for generating helper-dependent adenoviral vectors. *Molecular Therapy*, *3*, (5 Pt 1), 809–815. http://www.ncbi.nlm.nih.gov/entrez/query.fcgi?cmd=Retrieve&db=PubMed&dopt=Citation&list_uids=11356086
12. Phillips, S., Ramos, P. V., Veeraraghavan, P., & Young, S. M. (2022). VikAD, a Vika site-specific recombinase-based system for efficient and scalable helper-dependent adenovirus production. *Molecular Therapy – Methods and Clinical Development*, *24*, 117–126. https://doi.org/10.1016/j.omtm.2021.12.001
13. Ng, P., Evelegh, C., Cummings, D., & Graham, F. L. (2002). Cre levels limit packaging signal excision efficiency in the Cre/loxP helper-dependent adenoviral vector system. *Journal of Virology*, *76*(9), 4181–4189. http://www.ncbi.nlm.nih.gov/entrez/query.fcgi?cmd=Retrieve&db=PubMed&dopt=Citation&list_uids=11932383.[CrossRef]
14. Loonstra, A., Vooijs, M., Beverloo, H. B., Allak, B. Al, Van Drunen, E., Kanaar, R., Berns, A., & Jonkers, J. (2001). Growth inhibition and DNA damage induced by Cre recombinase in mammalian cells. *Proc. Natl. Acad. Sci. U.S.A.*, *98*(16), 9209–9214. https://doi.org/10.1073/pnas.161269798
15. Baba, Y., Nakano, M., Yamada, Y., Saito, I., & Kanegae, Y. (2005). Practical range of effective dose for Cre recombinase-expressing recombinant adenovirus without cell toxicity in mammalian cells. *Microbiology and Immunology*, *49*(6), 559–570. https://doi.org/10.1111/j.1348-0421.2005.tb03753.x
16. Duarte Azevedo, M., Sander, S., Jeanneret, C., Olfat, S., & Tenenbaum, L. (2021). Selective targeting of striatal parvalbumin-expressing interneurons for transgene delivery. *Journal of Neuroscience Methods*, *354*, (October 2020), 109105. https://doi.org/10.1016/j.jneumeth.2021.109105
17. Schmidt, E. E., Taylor, D. S., Prigge, J. R., Barnett, S., & Capecchi, M. R. (2000). Illegitimate Cre-dependent chromosome rearrangements in transgenic mouse spermatids. *Proc. Natl. Acad. Sci. U.S.A.*, *97*(25), 13702–13707. https://doi.org/10.1073/pnas.240471297
18. Harno, E., Cottrell, E. C., & White, A. (2013). Metabolic pitfalls of CNS cre-based technology. *Cell metabolism*, *18*(1), 21–28. https://doi.org/10.1016/j.cmet.2013.05.019
19. Gonzalez-Aparicio, M., Mauleon, I., Alzuguren, P., Bunuales, M., Gonzalez-Aseguinolaza, G., San Martin, C., Prieto, J., & Hernandez-Alcoceba, R. (2011). Self-inactivating helper virus for the production of high-capacity adenoviral vectors. *Gene Therapy*, *18*(11), 1025–1033. https://doi.org/10.1038/gt.2011.58
20. Jullien, N. (2003). Regulation of Cre recombinase by ligand-induced complementation of inactive fragments. *Nucleic acids research*, *31*(21), 131e–131. https://doi.org/10.1093/nar/gng131
21. Rajaee, M., & Ow, D. W. (2017). A new location to split Cre recombinase for protein fragment complementation. *Plant Biotechnology Journal*, *15*(11), 1420–1428. https://doi.org/10.1111/pbi.12726
22. Sauer, B., & Henderson, N. (1990). Targeted insertion of exogenous DNA into the eukaryotic genome by the Cre recombinase. *The New Biologist*, *2*(5), 441–449.
23. He, T. C., Zhou, S., da Costa, L. T., Yu, J., Kinzler, K. W., & Vogelstein, B. (1998). A simplified system for generating recombinant adenoviruses. *Proc. Natl. Acad. Sci. U.S.A.*, *95*(5), 2509–2514. http://www.ncbi.nlm.nih.gov/entrez/query.fcgi?cmd=Retrieve&db=PubMed&dopt=Citation&list_uids=9482916.[CrossRef]
24. Chen, L., Anton, M., & Graham, F. L. (1996). Production and characterization of human 293 cell lines expressing the site-specific recombinase Cre. *Somat Cell Mol Genet*, *22*(6), 477–488. http://www.ncbi.nlm.nih.gov/entrez/query.fcgi?cmd=Retrieve&db=PubMed&dopt=Citation&list_uids=9131017
25. Sweeney, J. A., & Hennessey, J. P. (2002). Evaluation of accuracy and precision of adenovirus absorptivity at 260 nm under conditions of complete DNA disruption. *Virology*, *295*(2), 284–288. https://doi.org/10.1006/viro.2002.1406
26. Gibb, B., Gupta, K., Ghosh, K., Sharp, R., Chen, J., & van Duyne, G. D. (2010). Requirements for catalysis in the Cre recombinase active site. *Nucleic acids research*, *38*(17), 5817–5832. https://doi.org/10.1093/nar/gkq384
27. Roberts, B. (1989). Nuclear location signal-mediated protein transport. *BBA – Gene Structure and Expression*, *1008*(3), 263–280. https://doi.org/10.1016/0167-4781(89)90016-X
28. Le, Y., Gagneten, S., Tombaccini, D., Bethke, B., & Sauer, B. (1999). Nuclear targeting determinants of the phage P1 Cre DNA recombinase. *Nucleic acids research*, *27*(24), 4703–4709. https://doi.org/10.1093/nar/27.24.4703
29. Duyne, G. D. Van (2001). a s tructural v iew of cre-loxp s ite -s pecific r ecombination. *Annual Review of Biophysical and Biomolecular Structure*, *1*(58), 87–104.
30. Palmer, D., & Ng, P. (2003). Improved system for helper-dependent adenoviral vector production. *Molecular Therapy*, *8*(5), 846–852. https://doi.org/10.1016/j.ymthe.2003.08.014
31. Tapia, F., Vázquez-Ramírez, D., Genzel, Y., & Reichl, U. (2016). Bioreactors for high cell density and continuous multi-stage cultivations: Options for process intensification in cell culture-based viral vaccine production. *Applied Microbiology and Biotechnology*, *100*(5), 2121–2132. https://doi.org/10.1007/s00253-015-7267-9
32. Suzuki, M., Cela, R., Clarke, C., Bertin, T. K., Mourino, S., & Lee, B. (2010). Large-scale production of high-quality helper-dependent adenoviral vectors using adherent cells in cell factories. *Human Gene Therapy*, *21*(1), 120–126. https://doi.org/10.1089/hum.2009.096
33. Mitani, K., Grahamt, F. L., Caskey, C. T., & Thomas, C., Kochanek, S. (2022). Rescue, Propagation, and Partial Purification of a Helper Virus-Dependent Adenovirus Vector. *Proc. Natl. Acad. Sci. U.S.A.*, *92*(9), 3854–3858.
34. Saha, B., Wong, C. M., & Parks, R. J. (2014). The adenovirus genome contributes to the structural stability of the virion. *Viruses*, *6*(9), 3563–3583. https://doi.org/10.3390/v6093563

SUPPORTING INFORMATION

Additional supporting information can be found online in the Supporting Information section at the end of this article.

How to cite this article: Gonzalez-Aparicio, M., Bunuales, M., de Landazuri, I. O., Prieto, J., & Hernandez-Alcoceba, R. (2023). Application of a split-Cre system for high-capacity adenoviral vector amplification. *Biotechnology Journal*, *18*, e2200227. https://doi.org/10.1002/biot.202200227